

GPO PRICE \$ _____

OTS PRICE(S) \$ _____

NASAHard copy (HC) 2.00Microfiche (MF) .50**MEMORANDUM**

FREE-FLIGHT INVESTIGATION OF THE
 DRAG OF A 60° DELTA-WING CONFIGURATION WITH LARGE
 STORES MOUNTED BELOW THE INDENTED FUSELAGE AT
 MACH NUMBERS BETWEEN 0.8 AND 1.6

By Sherwood Hoffman

Langley Research Center
 Langley Field, Va.

Authority: Memo Geo. Drobka NASA HQ.
 Code ATSS-A Dtd. 3-12-64 Subj: Change
 in Security Classification Marking.

**NATIONAL AERONAUTICS AND
 SPACE ADMINISTRATION**

WASHINGTON

October 1958

(THRU)

(CODE)

(CATEGORY)

(PAGES)

(NASA CR OR TMX OR AD NUMBER)

65-12123
 31

CONFIDENTIAL

NATIONAL AERONAUTICS AND SPACE ADMINISTRATION

NASA MEMO 10-9-58L

FREE-FLIGHT INVESTIGATION OF THE
DRAG OF A 60° DELTA-WING CONFIGURATION WITH LARGE
STORES MOUNTED BELOW THE INDENTED FUSELAGE AT
MACH NUMBERS BETWEEN 0.8 AND 1.6*

By Sherwood Hoffman

SUMMARY

Free-flight tests near zero lift were conducted between Mach numbers 0.8 and 1.6 to determine the drag of a 60° delta-wing configuration with large stores under the fuselage. The fuselage was indented for $M = 1.0$ to cancel only the wing areas. Three finned stores with fineness ratios of 8, 10, and 12 and with equal volume were mounted on struts and tested in the region of the fuselage indentation. The vertical displacement of the stores was held constant. Small-scale models of the isolated stores also were tested.

Increasing the store fineness ratio from 8 to 10 to 12 resulted in successive reductions in total drag. Unfavorable interference effects were obtained from each store through the Mach number range except for the fineness-ratio-12 store at the higher supersonic Mach numbers. The agreement obtained between the measured pressure drags and those calculated from the supersonic-area-rule theory ranged from good to poor for the models with stores.

INTRODUCTION

In general, previous store investigations have been limited to external-store installations that were suitable for mounting on wings. For example, references 1 and 2 present detailed studies of the interference effects from external stores (or nacelles) in a large number of positions about sweptback and delta wings. When a very large store or

*Title, Unclassified.

DECLASSIFIED - EFFECTIVE 1-15-64
Authority: Memo Geo. Drobka NASA HQ.
Code ATSS-A Dtd. 3-12-64 Subj: Change
in Security Classification Marking

12723

Author

037102 [REDACTED]

bomb is desired, it may be necessary to mount the store on the fuselage, especially on airplanes having thin and low-aspect-ratio wings.

The present investigation was conducted to determine the drag of a 60° delta-wing configuration with large strut-mounted stores located below the fuselage. The fuselage had a symmetrical Mach number 1.0 indentation for the wing alone in order to minimize the sonic drag rise (ref. 3) of the wing-body combination. Three finned stores of fineness ratios 8, 10, and 12 and equal volume were tested in the region of the fuselage indentation. The lengths of the stores were approximately equal to 43, 50, and 56 percent of the fuselage length, respectively. In addition, small models of the isolated stores were tested to determine the interference between the stores and wing-body configuration.

The models with stores were rocket-propelled vehicles which were tested (at approximately zero lift) through a range of Mach number from 0.8 to 1.6 and corresponding Reynolds number, based on wing mean aerodynamic chord, from about 7×10^6 to 18×10^6 .

SYMBOLS

A	cross-sectional area, sq ft
a_z	longitudinal acceleration, ft/sec ²
C_D	total drag coefficient based on S_w
$C_{D,f}$	friction drag coefficient based on S_w
$C_{D,v}$	total drag coefficient of isolated store based on $v^{2/3}$
$C_{D,v,f}$	friction drag coefficient of isolated store based on $v^{2/3}$
ΔC_D	pressure drag coefficient, $C_D - C_{D,f}$
$\Delta C_{D,v}$	pressure drag coefficient of isolated store, $C_{D,v} - C_{D,v,f}$
n	fineness ratio
g	acceleration due to gravity, 32.2 ft/sec ²
L	length of fuselage, ft

[REDACTED]

l	length of stores, ft
M	free-stream Mach number
N	number of terms in Fourier series
q	free-stream dynamic pressure, lb/sq ft
R	Reynolds number based on wing mean aerodynamic chord
r	radius, ft
S_w	total wing plan-form area, sq ft
W	weight, lb
V	volume of store, cu ft
X	station measured from fuselage nose, ft
x	station measured from store nose, ft
γ	elevation angle of flight path, deg
ϕ	roll angle, deg

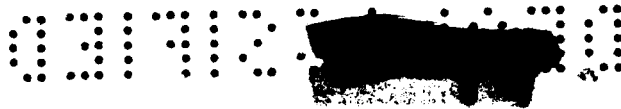
$$\beta = \sqrt{M^2 - 1}$$

MODELS

A list of the models tested, including one model from reference 4, and their designations are given in table I. Details and dimensions of all the configurations and stores are presented in figures 1 to 3 and tables II to IV. The normal cross-sectional-area distributions and photographs of the models are shown in figures 4 and 5, respectively.

The indented-wing-body configuration (model A) was derived from model 3 of reference 4 by indenting the fuselage symmetrically to cancel the exposed normal cross-sectional areas of the wing. The original configuration consisted of a 60° delta wing with an NACA 65A003 airfoil section in the free-stream direction, a fineness-ratio-10 parabolic fuselage, and two thin 60° sweptback stabilizing fins in the vertical plane.





Models B, C, and D consisted of the indented-wing-body configuration (model A) with large stores of fineness ratios 8, 10, and 12, respectively, mounted on struts below the fuselage. The midpoint of the stores and struts was located at a longitudinal station which corresponded to the quarter-chord station of the wing mean aerodynamic chord. The vertical position of the stores was kept constant, but the minimum clearance between the stores and fuselage varied as the store fineness ratio was increased. The minimum clearance was 0.21, 0.26, and 0.32 of the store maximum diameter, respectively, for the stores with fineness ratios of 8, 10, and 12. Each store had four symmetrically mounted 45° swept-back fins.

The stores were designed in the manner described in reference 5 to be minimum-wave-drag bodies of revolution with cylindrical center sections. The volume and ratio of total length to cylinder length were kept constant. The lengths of the stores, in order of increasing fineness ratio, were about 43, 50, and 56 percent of the fuselage length. Each store had a volume which was approximately equal to 16 percent of the fuselage volume. The strut had a thickness ratio of 6 percent and a section which consisted of an elliptical leading edge, a flat midsection, and a wedge trailing edge.

The isolated store models were 0.308-scale models of the stores tested on the configuration. Models E, F, and G correspond to the stores of fineness ratios 8, 10, and 12, respectively.

TEST TECHNIQUE

All the models were tested at the Langley Pilotless Aircraft Research Station at Wallops Island, Va. Models A to D were boosted to their maximum test Mach numbers by single-stage fin-stabilized rocket motors. A 5-inch HVAR booster was used for model A and 6-inch ABL Deacon rocket motors were utilized for models B, C, and D. Model C and the booster in launching position are shown in figure 5(h). After burnout of the booster rocket fuel, the higher drag-weight ratio of the booster, as compared with that of the model, allowed the model to separate longitudinally from the booster. The isolated store models E, F, and G were propelled to supersonic speeds from a helium gun which is described in reference 6. Velocity and trajectory data were obtained from the CW Doppler velocimeter and the NACA modified SCR-584 tracking radar unit, respectively. A survey of atmospheric conditions including winds aloft was made from an ascending balloon that was released at the time of each launching.



CONFIDENTIAL

DATA REDUCTION, ACCURACY, AND ANALYSIS

All the data were recorded and analyzed during coasting flight as the models, free from their boosters, decelerated through the Mach number ranges reported. For models A to D, the total drag coefficient was evaluated from the expression

$$C_D = - \frac{W}{gqS_w} (a_z + g \sin \gamma)$$

where a_z was obtained by differentiating the velocity-time curve from the CW Doppler radar unit. The values of q and γ were obtained from the measurements of tangential velocity and atmospheric conditions along the trajectory of each model. The drag coefficients $C_{D,v}$ for the isolated stores (models E, F, and G) were determined in the same manner but were based on $V^2/3$ in order to compare the store drags on an equal-volume basis. These coefficients also were based on S_w adjusted for model scale for comparison with C_D from the corresponding wing-body-store models. The error in total drag coefficient, based on S_w , was estimated to be less than ± 0.0007 throughout the Mach number range. The Mach numbers were determined within ± 0.01 throughout the test range.

The experimental pressure drag coefficient (ΔC_D or $\Delta C_{D,v}$) for each model was obtained by subtracting an estimated friction drag coefficient from the total drag at corresponding Mach numbers. The friction drag variation through the Mach number range was determined by adjusting the subsonic drag level of each model for Reynolds number effect with the use of the equations of Van Driest (ref. 7). For the variations of skin friction with Reynolds number, it was assumed that the boundary layer over the fuselage and stores was turbulent and that transition occurred at the 30-percent-chord station of the wing and at the 50-percent-chord station of the struts and fins. No adjustments were made for the base drag rise of any of the models. Reference 4, however, indicates that for afterbodies similar to those used herein, the base drag rise is small.

The theoretical pressure drags were computed for all the models tested by using the supersonic area rule of reference 8. The computational procedure is described in reference 9. Since models B, C, and D were unsymmetrical in that the stores were mounted below the fuselage, it was necessary to determine the longitudinal distribution of the frontal projection of oblique areas cut by inclined Mach planes between roll

CONFIDENTIAL

03712: [REDACTED]

angles of 0° and 180° . The area distributions (the fuselage stabilizing fins being neglected) were determined graphically (see ref. 10) for every 15° of roll up to 180° . Models A, E, F, and G were symmetrical and only the areas between 0° and 90° of roll had to be considered. The Fourier sine series used for calculating the pressure drags was evaluated for 24 harmonics. Examples of the series solution at several values of $\beta \cos \phi$ for models A and C are shown in figure 6.

RESULTS AND DISCUSSION

The rocket-propelled models were tested through a range of Mach number from about 0.8 to 1.6. The corresponding Reynolds number varied from approximately 4×10^6 to 10×10^6 for the wing-body configuration (model A) and from about 7×10^6 to 18×10^6 for the models (models B, C, and D) with stores. The isolated store models (models E, F, and G), which were propelled from the helium gun, covered a Mach number range from about 0.95 to 1.3 with corresponding Reynolds numbers from approximately 3×10^6 to 6×10^6 . The Reynolds numbers are presented in figure 7 and are based on the wing mean aerodynamic chord adjusted for model scale.

The variations of total drag coefficient and friction drag coefficient for models A to D are presented in figure 8. The data from model A, which was a symmetrical configuration, are at zero lift. Models B, C, and D were unsymmetrical because of the mounting of the stores below the fuselage. The centers of gravity of these models were located to give static margins greater than one mean aerodynamic chord length. This condition resulted in very low trim lift coefficients for which the induced drag is negligible. (See, for example, ref. 11.) Calculations, which included the interference lift and drag as determined from linearized theory, indicated that the trim lift coefficient would be less than 0.03 (based on S_w) and the trim angle less than 0.8° at supersonic speeds.

The comparison of C_D in figure 8(a) shows a substantial increase in configuration drag due to the large underfuselage stores. The largest increase in drag, which was obtained from model B with the fineness-ratio-8 store, was approximately equal to 43 percent of the wing-body drag at high subsonic speeds and about 33 percent at supersonic speeds. Increasing the store fineness ratio resulted in successive reductions in drag, the largest reductions being obtained at the higher Mach numbers.

Figure 9 shows a breakdown of the total drag coefficients of each configuration with a store. The isolated-store drag coefficients and the strut drag coefficients (estimated from linearized theory) are based

[REDACTED]

on wing plan-form area in this figure. Up to about $M = 1.02$, the incremental drag between each model with a store and the model without a store (model A) is about twice as great as the sum of the drags from the corresponding isolated store and strut. At the higher Mach numbers, the incremental drag (store plus interference drag) for the models with the fineness-ratio-8 and -10 stores was slightly greater than the sum of the isolated store and strut drags, whereas the incremental drag for the configuration with the fineness-ratio-12 store was less than that for the isolated store and strut drag. In a similar investigation (ref. 12), the results also showed an unfavorable interference drag increment for a fineness-ratio-8.57 store mounted below the indented fuselage of a sweptback-wing configuration through a comparable Mach number range.

The theoretical pressure drags of models A to D are compared with the experimental pressure drags in figure 10. The comparisons show that the agreement between the supersonic area rule theory and experiment ranged from good for model A without stores and model C with the fineness-ratio-10 store to poor for model B with the fineness-ratio-8 store. A comparison of the increments in ΔC_D for model B (with the fineness-ratio-8 store) and model A (without a store) shows that the store-plus-interference pressure drags varied from one-third to one-half of the theoretical increment at supersonic speeds. For model D with the fineness-ratio-12 store, the theory gave a positive increment for the store whereas the test showed a small negative increment. In references 1, 13, and 14, where stores (or nacelles) were tested on wings of configurations having fuselage indentations, the agreement between the theory and experiment also varied from good to poor. It is evident that the area rule, which is a linearized theory, cannot account for all the interference effects, especially local interference effects.

The isolated-store drag coefficients are compared on an equal-volume basis in figure 11. As would be expected, the store total drag and pressure drag decreased with increasing fineness ratio at transonic and supersonic speeds. The area-rule theory, which was applied to each store with fins, gave unreasonably high values of pressure drag near $M = 1.0$ but fairly good agreement with the measured results above $M = 1.2$. The theoretical pressure drags of the stores without fins, as determined from reference 5, are also shown for comparison.

Figure 12 presents a comparison of the drags of the original configuration (ref. 4) and the indented configuration of the present investigation. The results are similar to those obtained for swept wings (ref. 15) and unswept wings (ref. 9) on fuselages indented for $M = 1.0$. Both the experimental results and the area-rule theory show that the transonic indentation becomes ineffective at low supersonic speeds and results in more total drag than was obtained from the original configuration above $M = 1.2$.

03710201930

CONCLUDING REMARKS

Free-flight tests were conducted to determine the drag, near zero lift, of a 60° delta-wing configuration with large stores mounted on struts below the fuselage between Mach numbers 0.8 and 1.6. The fuselage had an $M = 1.0$ indentation for the wing alone. The stores of fineness ratio 8, 10, and 12 and equal volume were tested separately in the region of the fuselage indentation. The vertical displacement of the stores was held constant.

Increasing the store fineness ratio from 8 to 10 to 12 resulted in successive reductions in total drag at transonic and supersonic speeds. Unfavorable interference effects were obtained from each store at high subsonic and transonic Mach numbers. The interference effects from each store at supersonic speeds were small relative to the corresponding isolated store drag with the configuration having the fineness-ratio-12 store experiencing some favorable interference effects. The agreement obtained between the measured pressure drags and those calculated from supersonic-area-rule theory ranged from good to poor for the models with stores.

Langley Research Center,
National Aeronautics and Space Administration,
Langley Field, Va., July 9, 1958.

REF ID: A66666

REFERENCES

1. Pearson, Albin O.: Transonic Investigation of Effects of Spanwise and Chordwise External Store Location and Body Contouring on Aerodynamic Characteristics of 45° Sweptback Wing-Body Configurations. NACA RM L57G17, 1957.
2. Morris, Odell A.: The Origin and Distribution of Supersonic Store Interference From Measurement of Individual Forces on Several Wing-Fuselage-Store Configurations. IV.- Delta-Wing Heavy-Bomber Configuration With Large Store. Mach Number, 1.61. NACA RM L55I27a, 1955.
3. Whitcomb, Richard T.: A Study of the Zero-Lift Drag-Rise Characteristics of Wing-Body Combinations Near the Speed of Sound. NACA Rep. 1273, 1956. (Supersedes NACA RM L52H08.)
4. Morrow, John D., and Nelson, Robert L.: Large-Scale Flight Measurements of Zero-Lift Drag of 10 Wing-Body Configurations at Mach Numbers From 0.8 to 1.6. NACA RM L52D18a, 1953.
5. Fuller, Franklyn B., and Briggs, Benjamin R.: Minimum Wave Drag of Bodies of Revolution With a Cylindrical Center Section. NACA TN 2535, 1951.
6. Hall, James Rudyard: Comparison of Free-Flight Measurements of the Zero-Lift Drag Rise of Six Airplane Configurations and Their Equivalent Bodies of Revolution at Transonic Speeds. NACA RM L53J21a, 1954.
7. Van Driest, E. R.: Turbulent Boundary Layer in Compressible Fluids. Jour. Aero. Sci., vol. 18, no. 3, Mar. 1951, pp. 145-160, 216.
8. Jones, Robert T.: Theory of Wing-Body Drag at Supersonic Speeds. NACA Rep. 1284, 1956. (Supersedes NACA RM A53H18a.)
9. Holdaway, George H.: Comparison of Theoretical and Experimental Zero-Lift Drag-Rise Characteristics of Wing-Body-Tail Combinations Near the Speed of Sound. NACA RM A53H17, 1953.
10. Nelson, Robert L., and Welsh, Clement J.: Some Examples of the Applications of the Transonic and Supersonic Area Rules to the Prediction of Wave Drag. NACA RM L56D11, 1956.

031713 [REDACTED]

11. Jacobsen, Carl R.: Effects of Size of External Stores on the Aerodynamic Characteristics of an Unswept and a 45° Sweptback Wing of Aspect Ratio 4 and a 60° Delta Wing at Mach Numbers of 1.41, 1.62, and 1.96. NACA RM L52K20a, 1953.
 12. Hoffman, Sherwood: Free-Flight Investigation at Mach Numbers From 0.8 to 1.5 of the Effect of a Fuselage Indentation on the Zero-Lift Drag of a 52.5° Sweptback-Wing—Body Configuration With Symmetrically Mounted Stores on the Fuselage. NACA RM L57L04, 1958.
 13. Petersen, Robert B.: Comparison of Experimental and Theoretical Zero-Lift Wave-Drag Results for Various Wing-Body-Tail Combinations at Mach Numbers Up to 1.9. NACA RM A56I07, 1957.
 14. Hoffman, Sherwood: Free-Flight Investigation of the Drag of a Model of a 60° Delta-Wing Bomber With Strut-Mounted Siamese Nacelles and Indented Fuselage at Mach Numbers From 0.80 to 1.35. NACA RM L57G29, 1957.
 15. Hoffman, Sherwood: A Flight Investigation of the Transonic Area Rule for a 52.5° Sweptback Wing-Body Configuration at Mach Numbers Between 0.8 and 1.6. NACA RM L54H13a, 1954.
- [REDACTED]

TABLE I.- MODELS

Model	Description
A	Wing + indented body
B	Wing + indented body + store (n = 8)
C	Wing + indented body + store (n = 10)
D	Wing + indented body + store (n = 12)
E	Isolated store, n = 8
F	Isolated store, n = 10
G	Isolated store, n = 12
Reference 4	Wing + parabolic body (model 3)

03710 000000

TABLE II.- FUSELAGE COORDINATES

$\frac{x}{L}$	r/L for -	
	Indented fuselage	Original fuselage
0.0000	0.0000	0.0000
.0154	.0038	.0038
.0308	.0074	.0074
.0615	.0142	.0142
.0923	.0204	.0204
.1231	.0260	.0260
.1538	.0311	.0311
.1846	.0355	.0355
.2154	.0394	.0394
.2462	.0426	.0426
.2769	.0453	.0453
.3078	.0473	.0473
.3385	.0488	.0488
.3692	.0497	.0497
.4000	.0500	.0500
.4308	.0499	.0499
.4497	.0498	.0498
.4863	.0486	.0495
.5289	.0463	.0488
.5716	.0433	.0479
.6095	.0402	.0469
.6474	.0368	.0457
.6948	.0337	.0439
.7327	.0323	.0423
.7699	.0322	.0404
.8133	.0342	.0381
.8370	.0366	.0367
.8615	.0351	.0351
.8923	.0331	.0331
.9231	.0309	.0309
.9538	.0286	.0286
.9846	.0261	.0261
1.0000	.0248	.0248

TABLE III.- COORDINATES OF NACA 65A003 AIRFOIL

[Stations measured from leading edge]

Station, percent chord	Ordinate, percent chord
0	0
.5	.234
.75	.284
1.25	.362
2.5	.493
5.0	.658
7.5	.796
10	.912
15	1.097
20	1.236
25	1.342
30	1.420
35	1.472
40	1.498
45	1.497
50	1.465
55	1.402
60	1.309
65	1.191
70	1.053
75	.897
80	.727
85	.549
90	.369
95	.188
100	.007
L.E. radius: 0.057 percent chord	
T.E. radius: 0.0068 percent chord	

03712 [REDACTED]

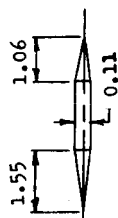
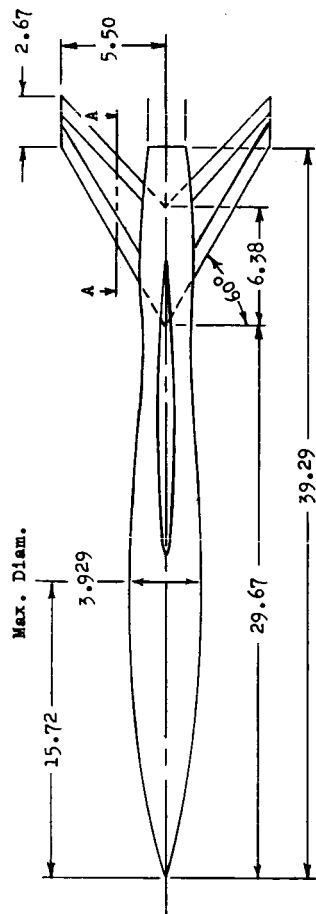
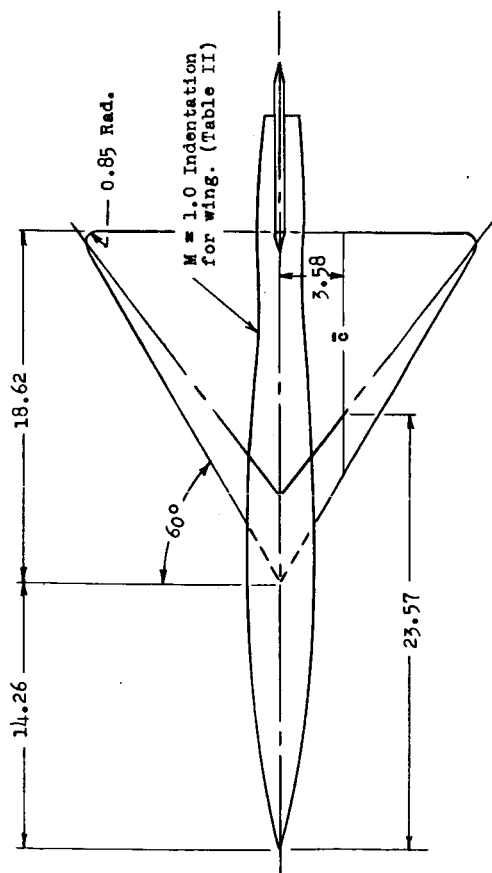
TABLE IV.- STORE COORDINATES

$\frac{x}{l}$	$\frac{r}{l}$ for stores with fineness ratios of -		
	8	10	12
0	0	0	0
.025	.0116	.0093	.0077
.05	.0185	.0148	.0123
.10	.0304	.0243	.0202
.15	.0392	.0314	.0262
.20	.0467	.0374	.0311
.25	.0522	.0418	.0348
.30	.0568	.0454	.0379
.35	.0601	.0481	.0401
.40	.0621	.0497	.0414
.422	.0625	.0500	.0417
.50	.0625	.0500	.0417
.578	.0625	.0500	.0417
.60	.0621	.0497	.0414
.65	.0601	.0481	.0401
.70	.0568	.0454	.0379
.75	.0522	.0418	.0348
.80	.0467	.0374	.0311
.85	.0392	.0314	.0262
.90	.0304	.0243	.0202
.95	.0185	.0148	.0123
.975	.0116	.0093	.0077
1.0	0	0	0

[REDACTED]

MODEL CHARACTERISTICS

Wing aspect ratio	2.31
Wing mean aerodynamic chord (\bar{c}), ft	1.03
Free-stream airfoil, NACA 65A003	Table III
Total wing plan-form area, sq ft	1.38
Fuselage fineness ratio	10.00
Fuselage frontal area, sq ft08



Section A-A
Typical fin section

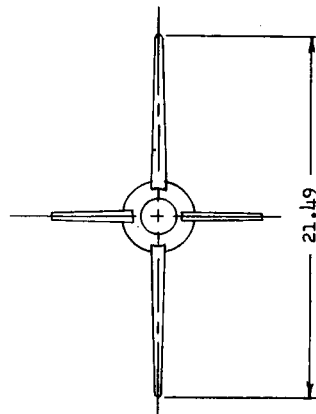
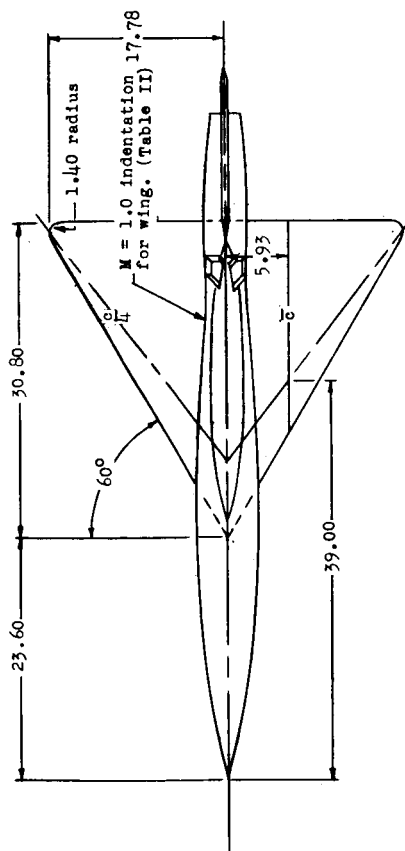


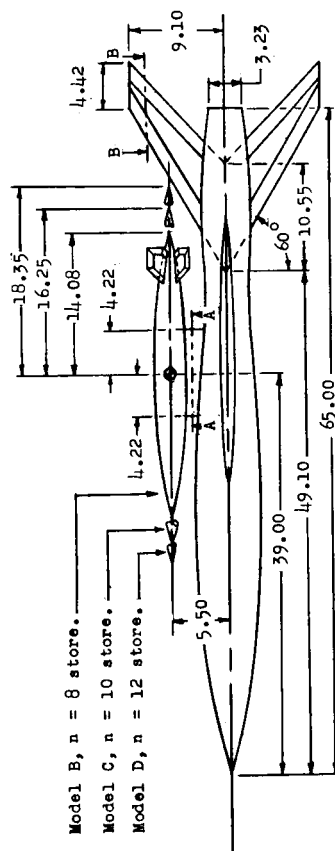
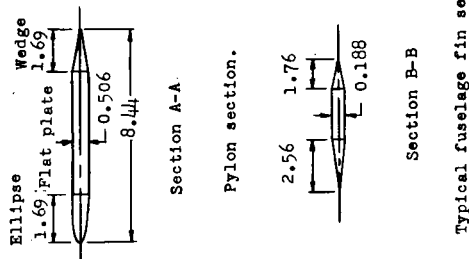
Figure 1.- Details and dimensions of the wing-body configuration with the fuselage indentation.
Model A. All dimensions are in inches unless otherwise noted.

MODEL CHARACTERISTICS

Wing aspect ratio	- - - - -	-
Wing mean aerodynamic chord (\bar{c}), ft.	- - - - -	2.31
Free-stream airfoil, NACA 65A003-	- - - - -	1.71
Total wing plan-form area, sq. ft.	- - - - -	Table III
Fuselage fineness ratio	- - - - -	3.78
Fuselage frontal area, sq. ft.-	- - - - -	10.00
Pylon thickness ratio	- - - - -	0.23
Fuselage frontal area, sq. ft.-	- - - - -	0.06

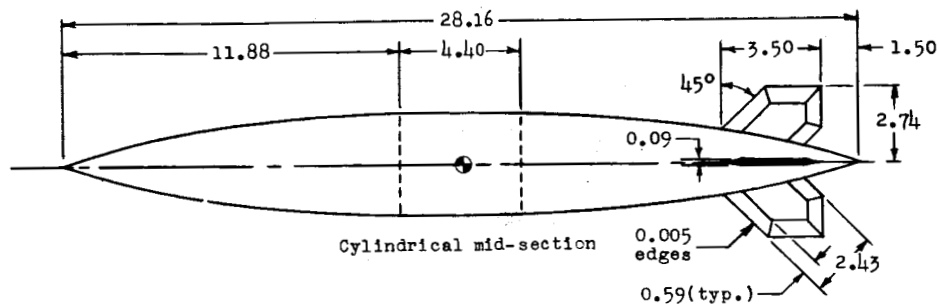


(a) Plan-form view of the model with the fineness-ratio-8 store. Model B.

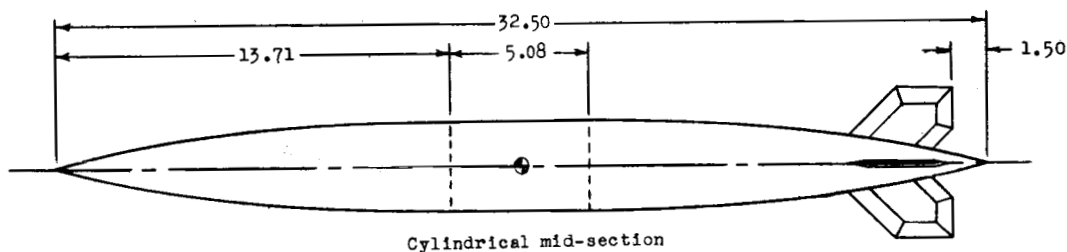


(b) Side view of model showing stores tested.
Models B, C, and D.

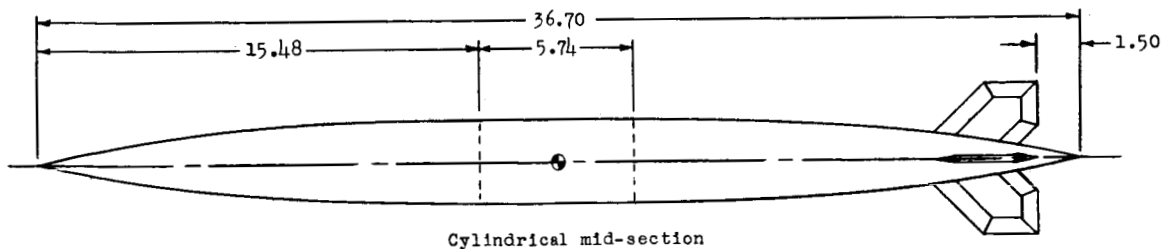
Figure 2.- Details and dimensions of models with stores. All dimensions are in inches unless otherwise noted.



(a) Fineness-ratio-8 store of model B.



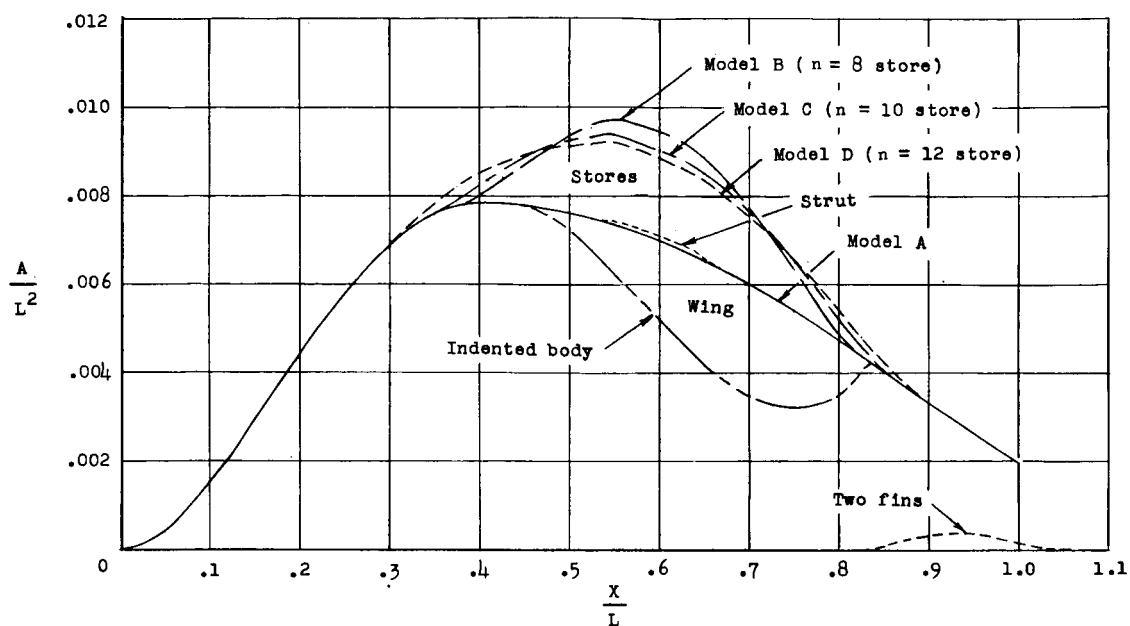
(b) Fineness-ratio-10 store of model C.



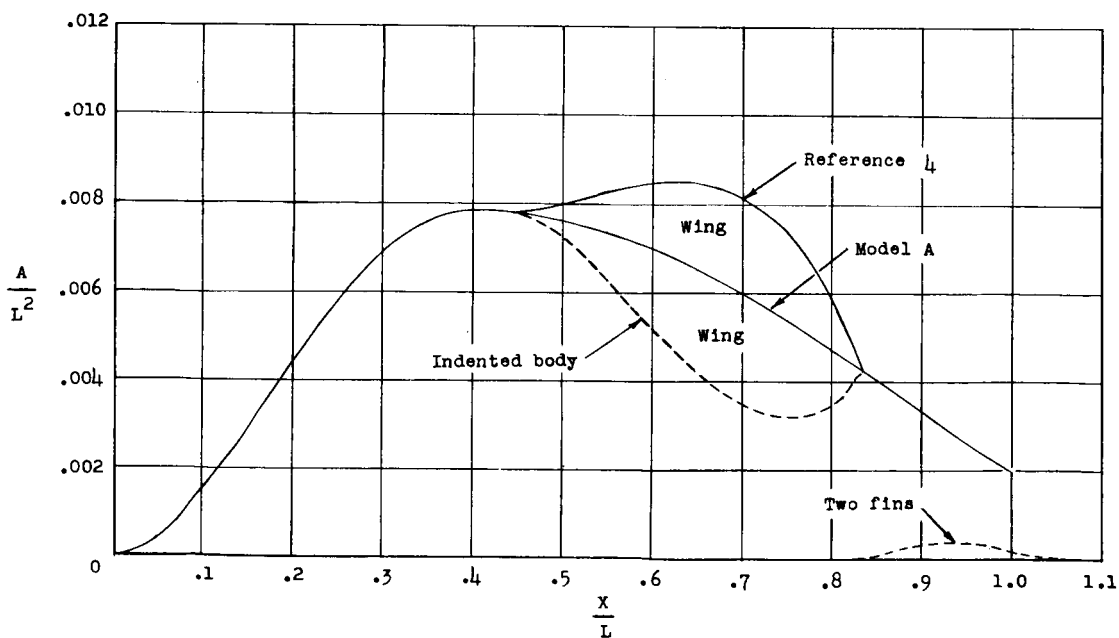
(c) Fineness-ratio-12 store of model D.

Figure 3.- Dimensions of stores tested on models B, C, and D. All dimensions are in inches. Store coordinates are given in table IV.

03710 [REDACTED]



(a) Wing-body-store models.

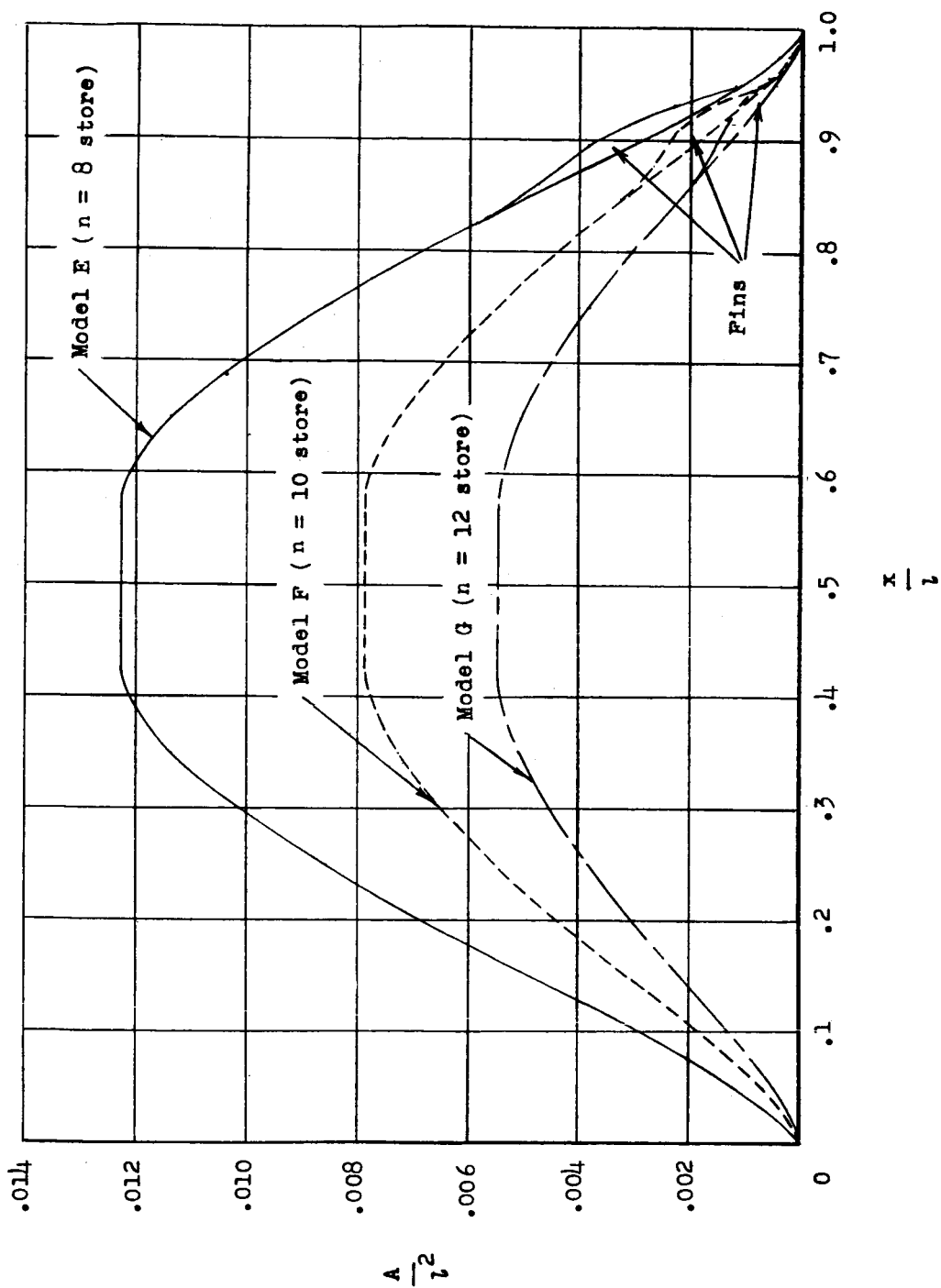


(b) Wing-body models.

Figure 4.- Normal cross-sectional area distributions of models tested.

[REDACTED]

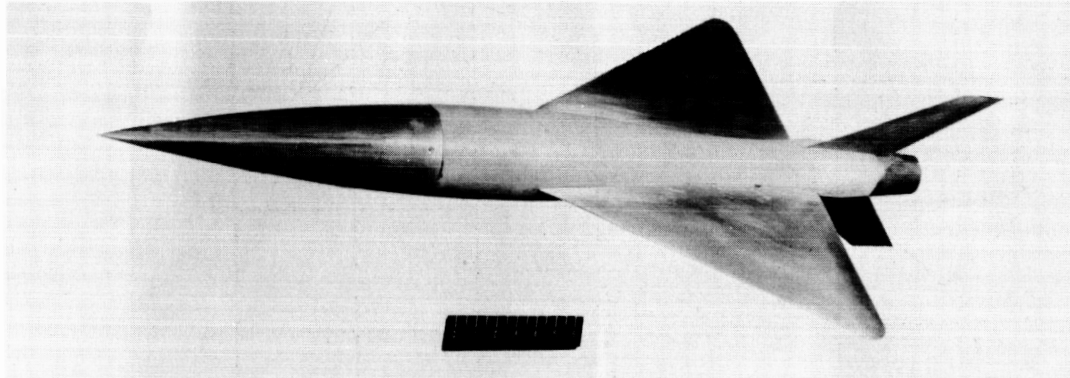
SECRET



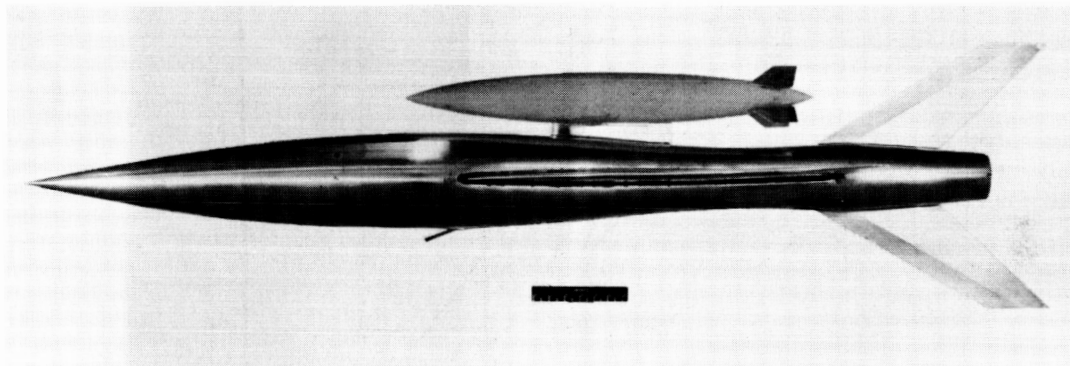
(c) Isolated stores.

Figure 4.- Concluded.

03712 [REDACTED]



(a) Model A.

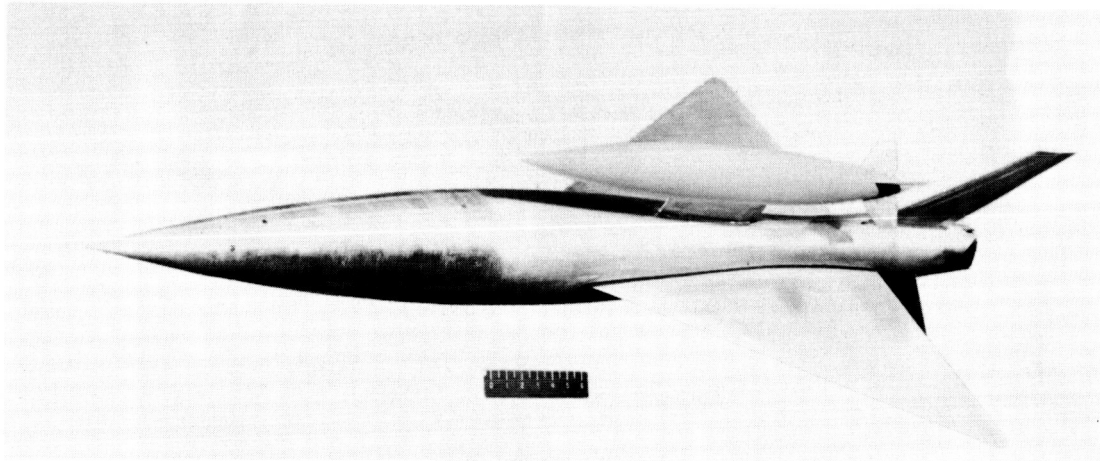


(b) Model B ($n = 8$ store).

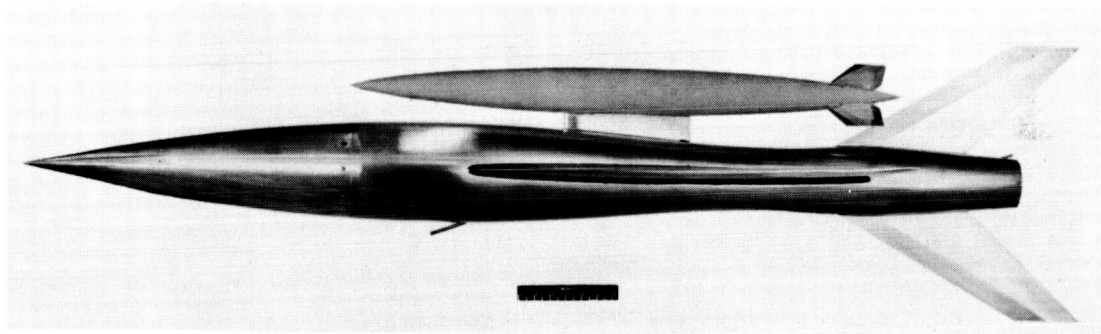
L-58-2510

Figure 5.- Photographs of models tested.

[REDACTED]



(c) Model C ($n = 10$ store).

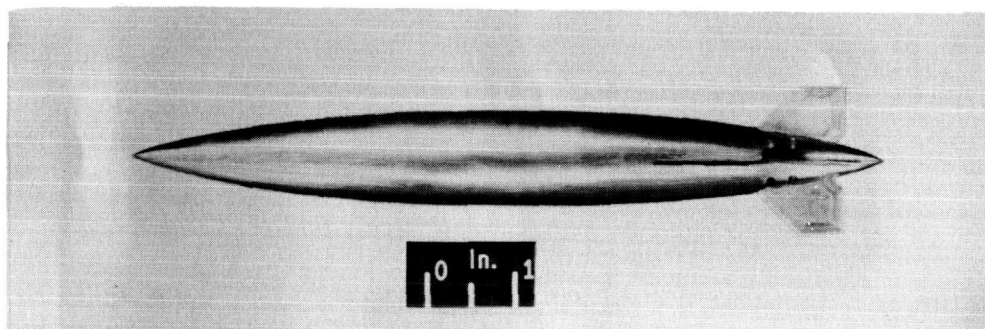


(d) Model D ($n = 12$ store).

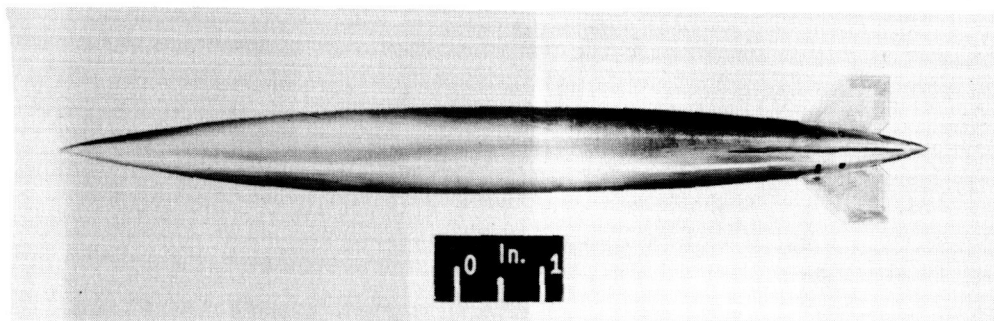
L-58-2511

Figure 5.- Continued.

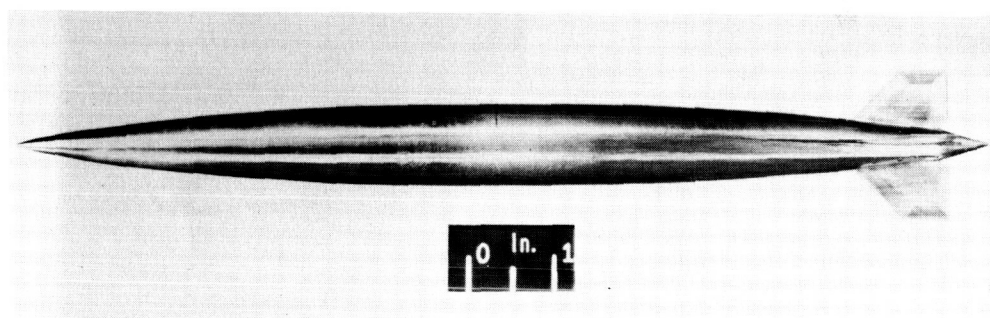
037123 [REDACTED]



(e) Model E ($n = 8$ store).



(f) Model F ($n = 10$ store).

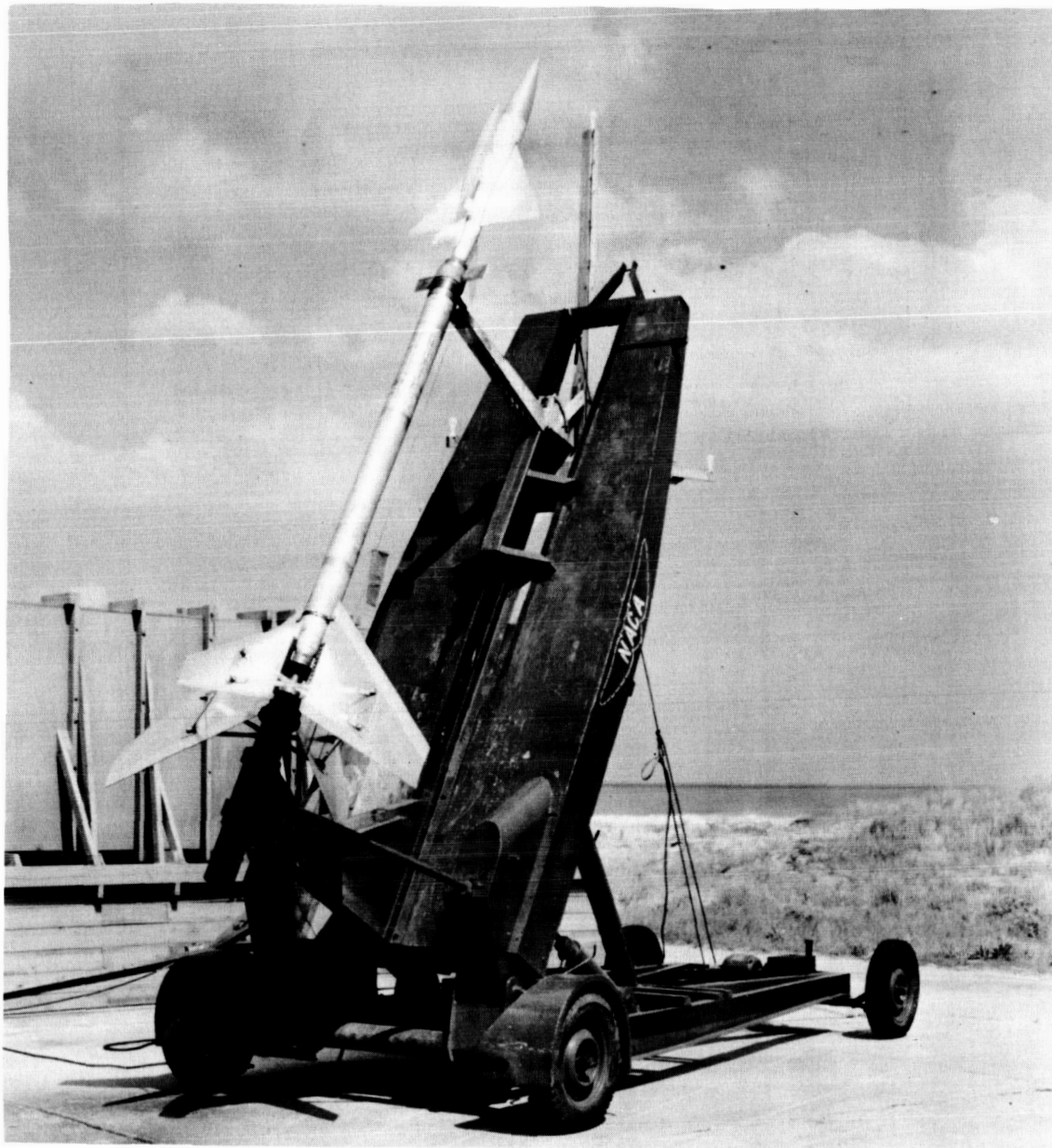


(g) Model G ($n = 12$ store).

L-58-2528

Figure 5.- Continued.

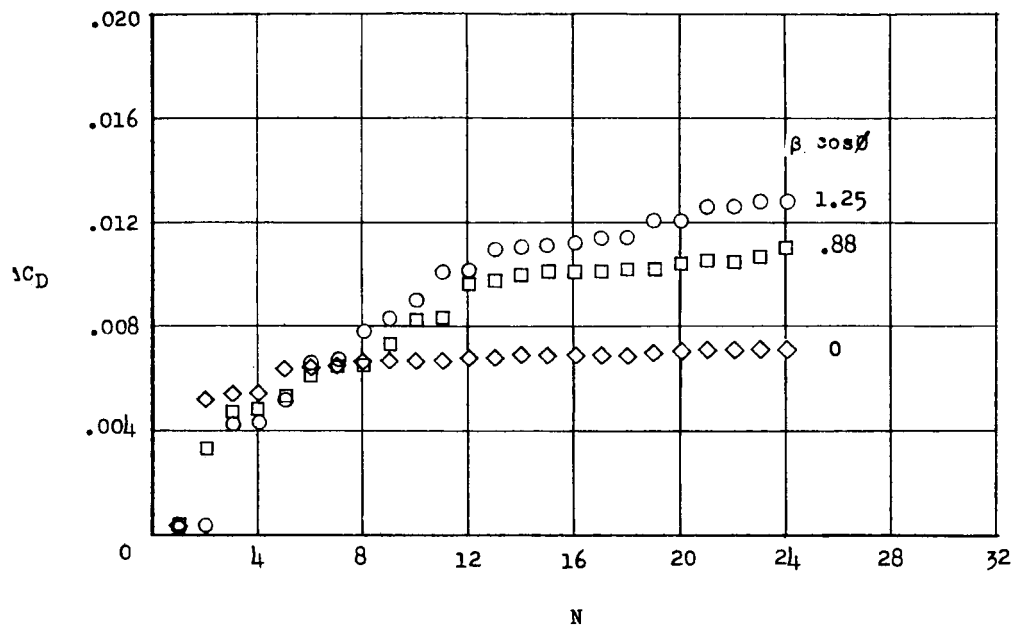
[REDACTED]



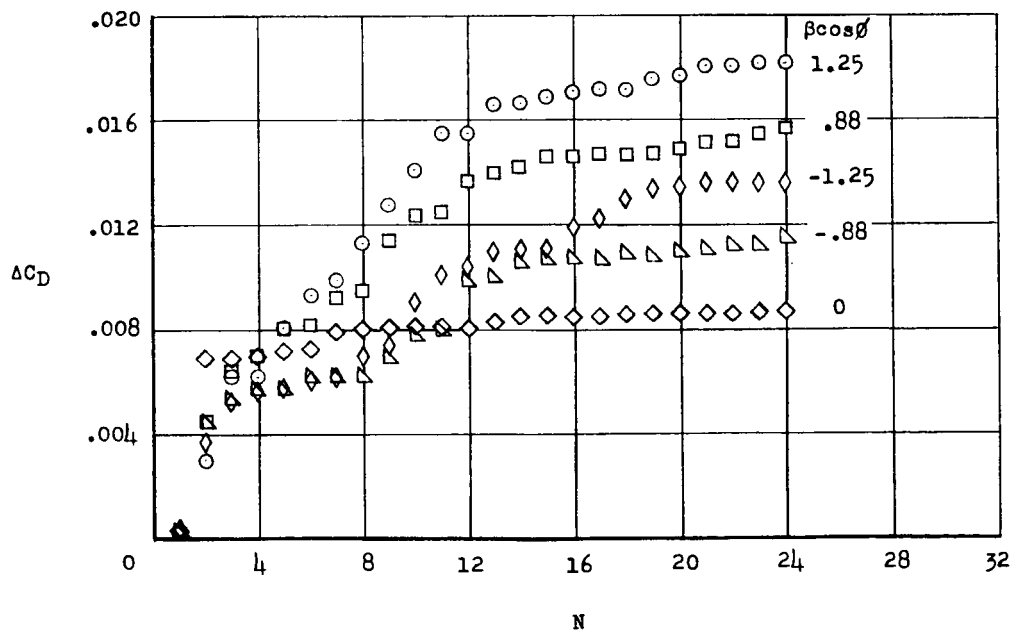
(h) Model C and booster on launcher. L-89647.1

Figure 5.- Concluded.

03712 [REDACTED]



(a) Model A.



(b) Model C.

Figure 6.- Examples of the Fourier series solution of ΔC_D for several values of $\beta \cos \phi$.

[REDACTED]

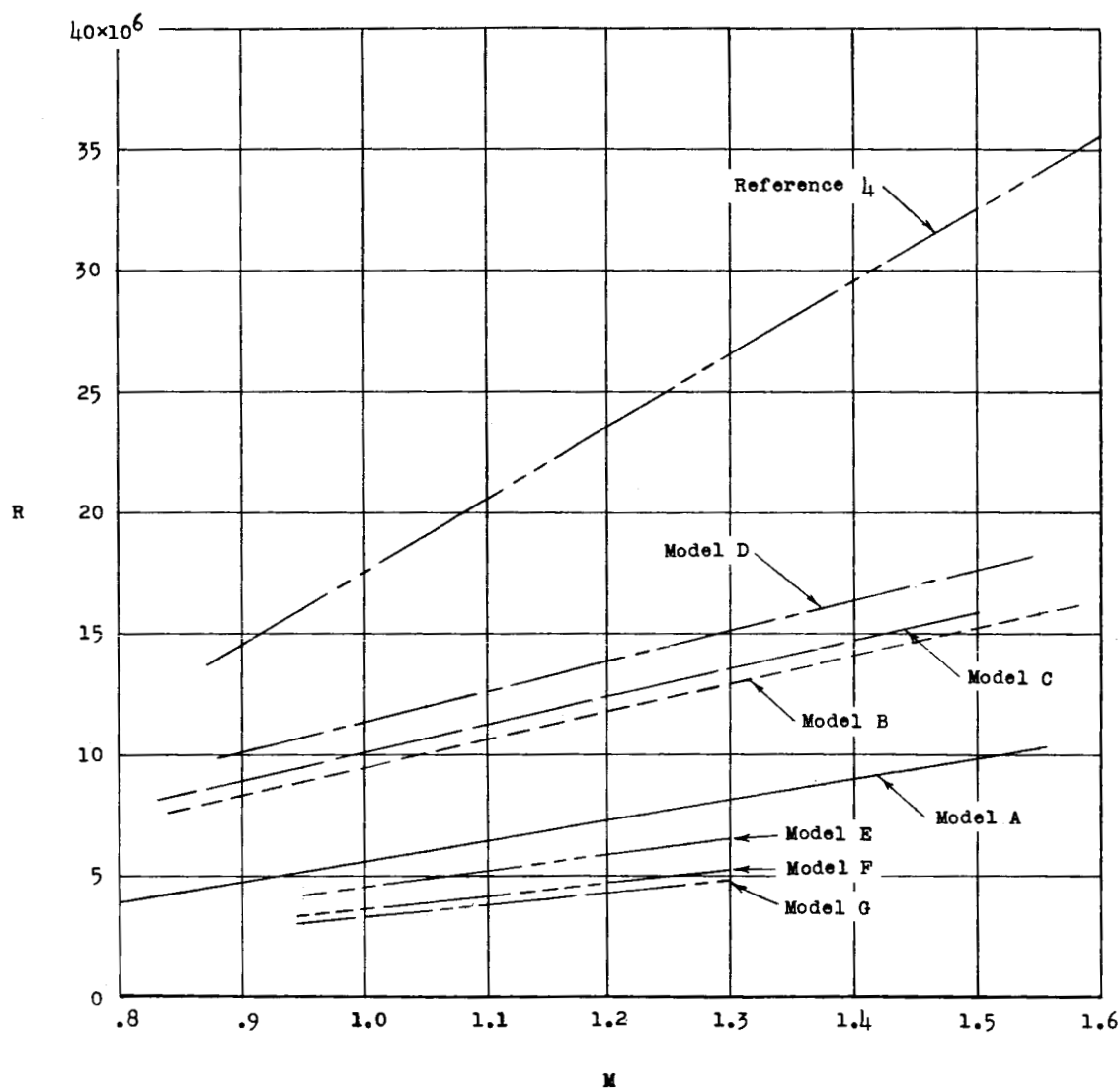
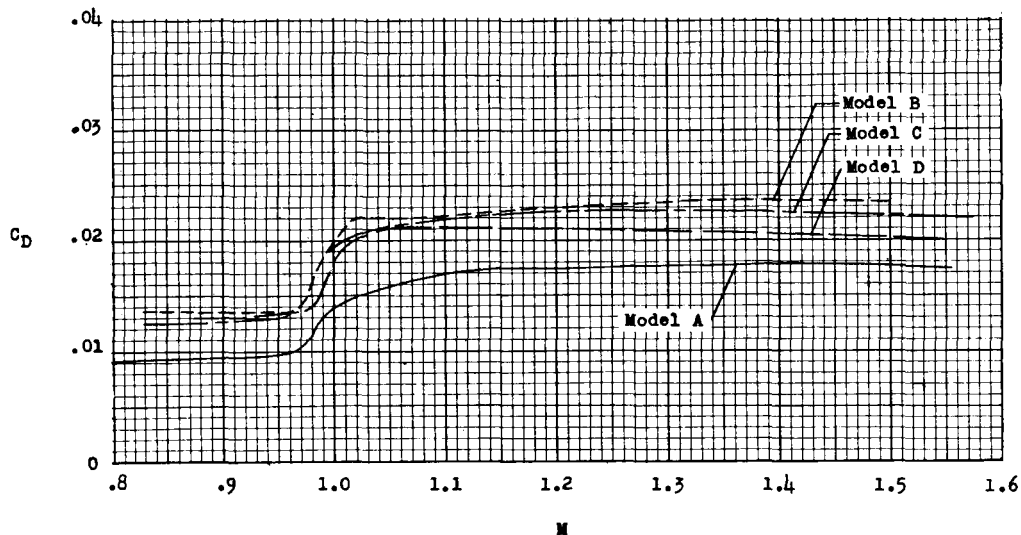
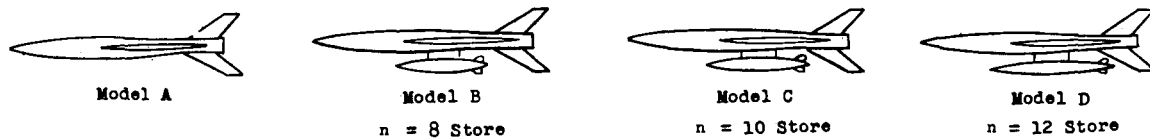
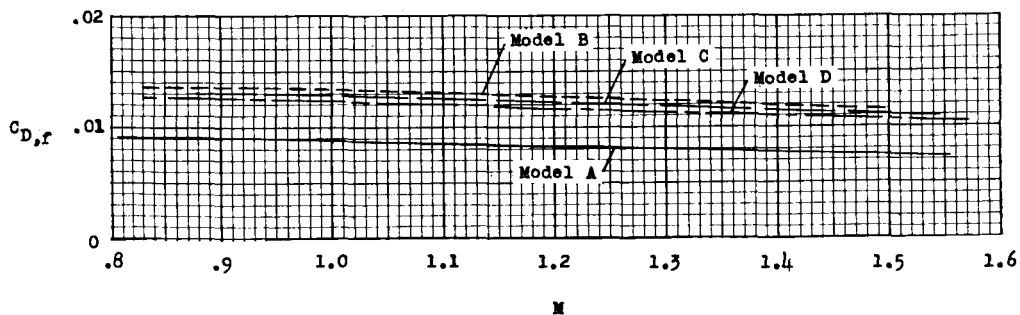


Figure 7.- Variation of Reynolds number with Mach number for models tested. Reynolds number is based on the wing mean aerodynamic chord adjusted for model scale.

03712 [REDACTED]

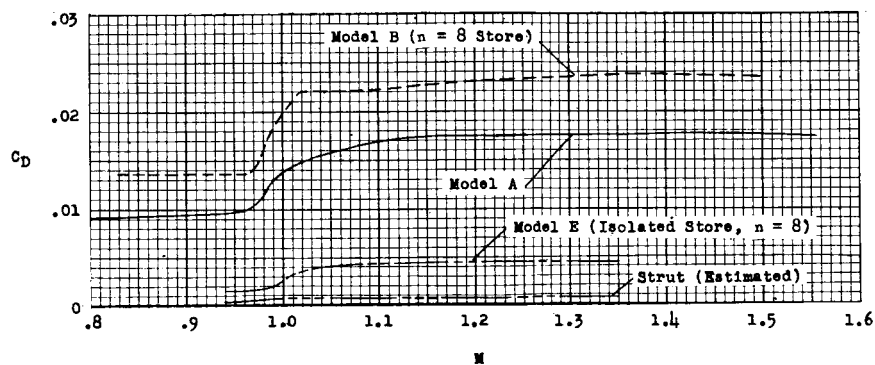


(a) Total drag coefficient.

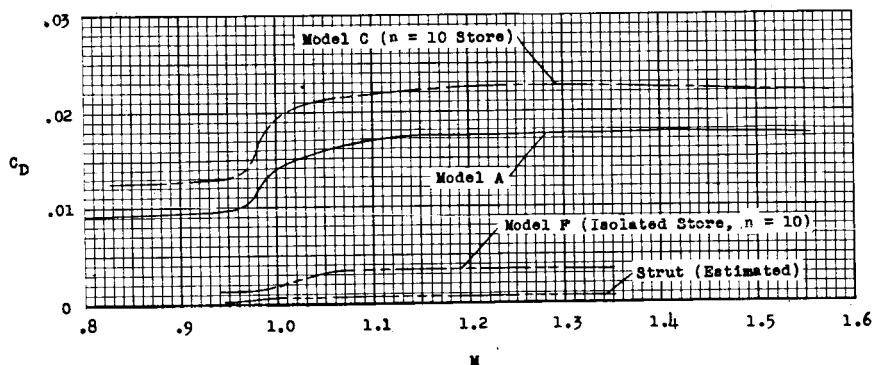


(b) Friction drag coefficient.

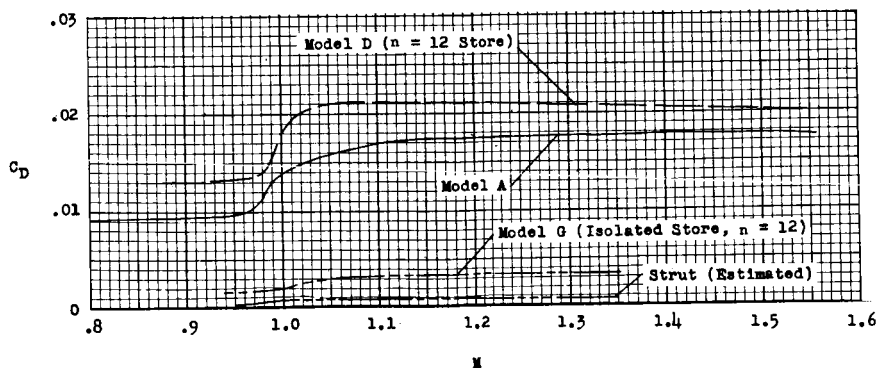
Figure 8.- Variations of total drag coefficient and friction drag coefficient for the indented models with and without stores.



(a) Wing-body combination with fineness-ratio-8 store.

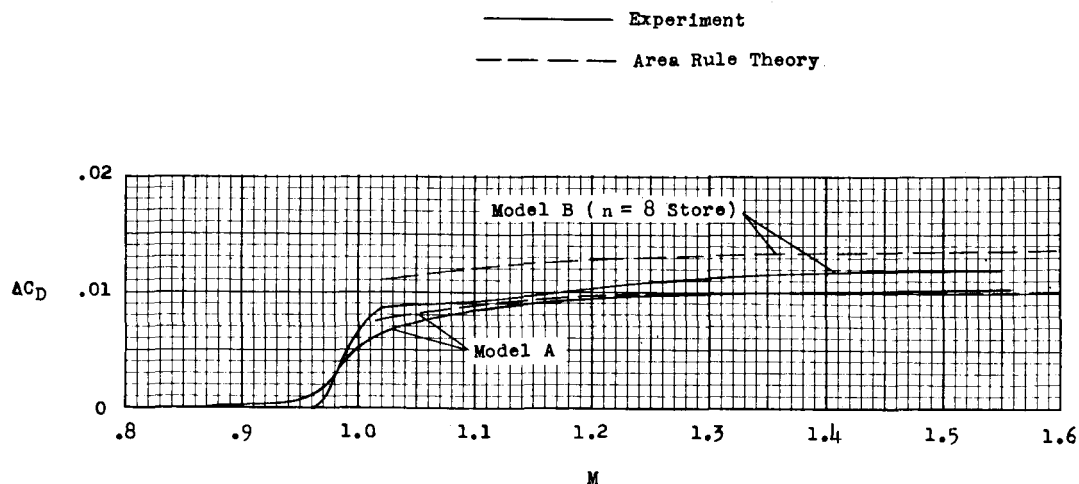


(b) Wing-body combination with fineness-ratio-10 store.

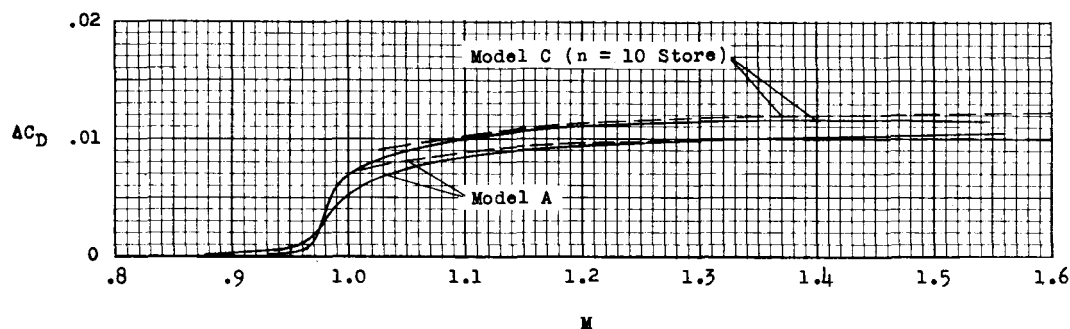


(c) Wing-body combination with fineness-ratio-12 store.

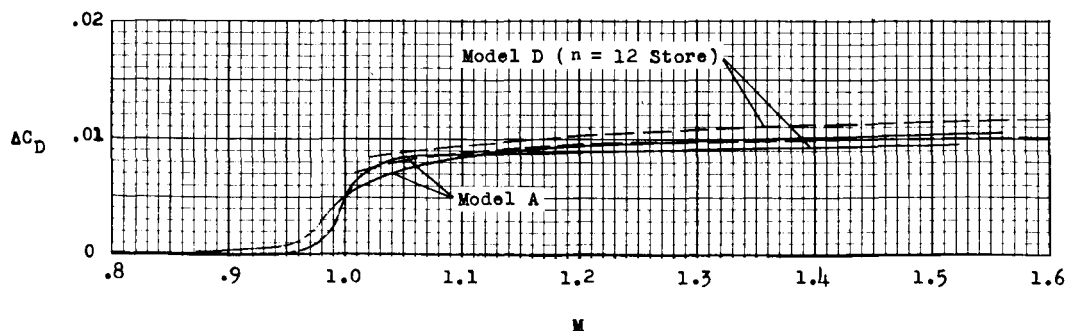
Figure 9.- Comparisons of the drag coefficients of the wing-body-store models and of the isolated store models.



(a) Wing-body combination with fineness-ratio-8 store.

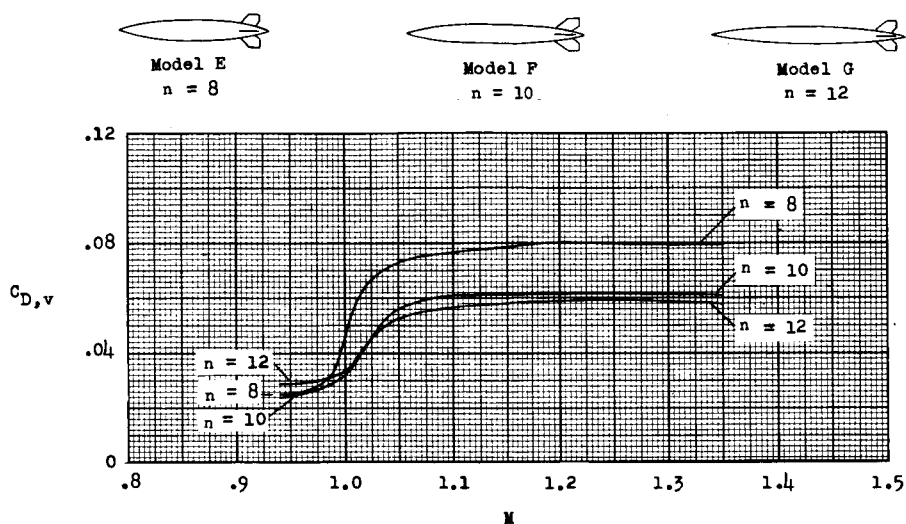


(b) Wing-body combination with fineness-ratio-10 store.

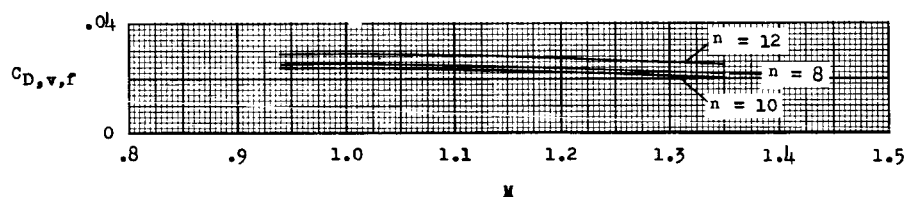


(c) Wing-body combination with fineness-ratio-12 store.

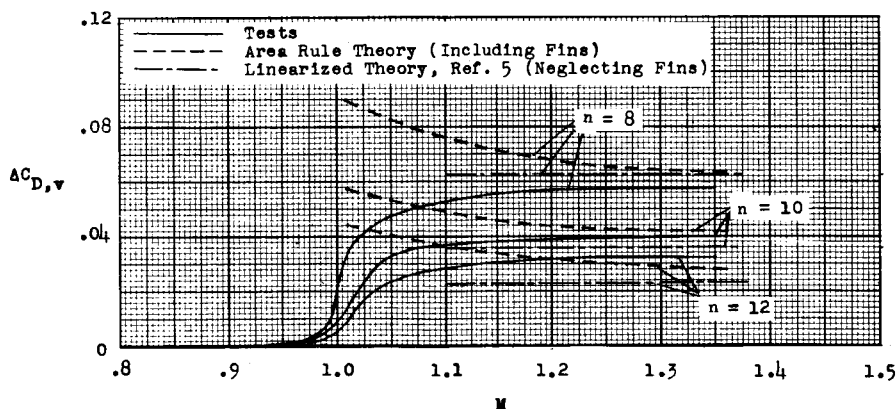
Figure 10.- Comparisons of the experimental and theoretical pressure-drag coefficients of the wing-body configurations with and without the stores.



(a) Total drag coefficients.

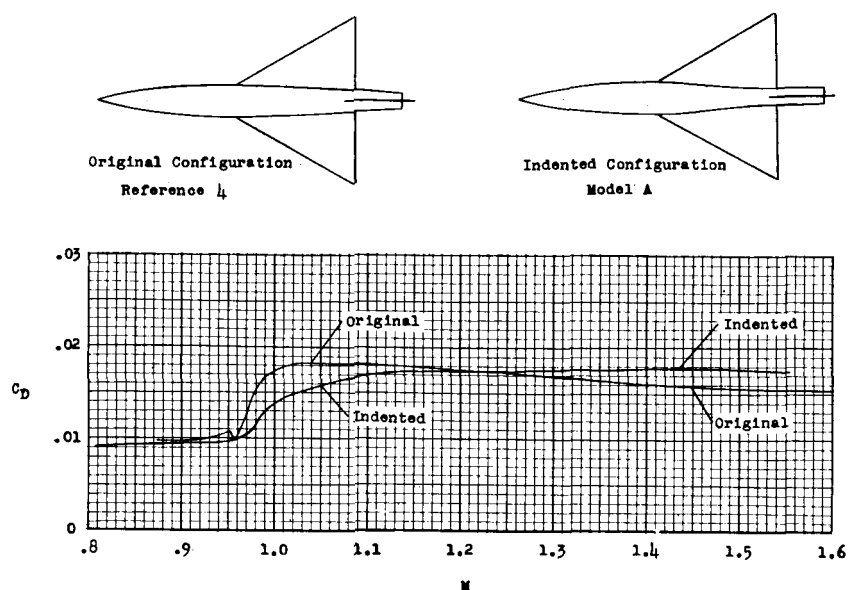


(b) Friction drag coefficients.

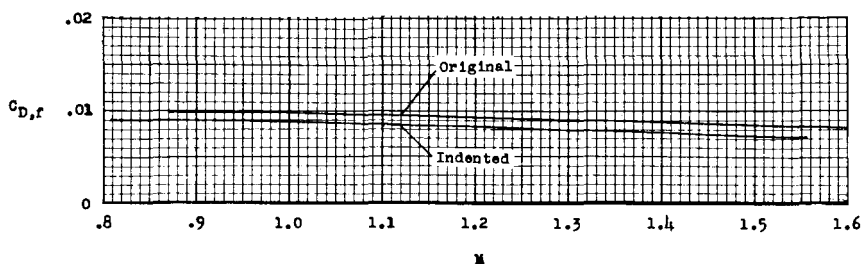


(c) Experimental and theoretical pressure drag coefficients.

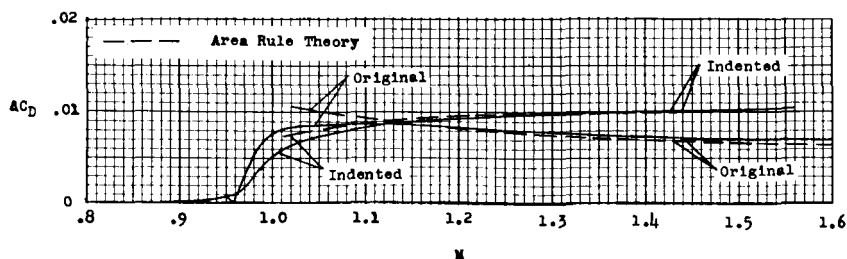
Figure 11.- Variations of the total drag coefficients, friction drag coefficients, and pressure drag coefficients with Mach number for the isolated store models.



(a) Total drag coefficients.



(b) Friction drag coefficients.



(c) Experimental and theoretical pressure drag coefficients.

Figure 12.- Comparisons of the total drag coefficients, friction drag coefficients, and pressure drag coefficients for the indented and the original parabolic fuselage-wing combinations.

